

Orientation of Spherical Janus Nanoparticles

Force and Torque Calculations due to an External Electric Field

J. van de Velde

Orientation of Spherical Janus Nanoparticles

Force and Torque Calculations due to an External Electric Field

by

J. van de Velde

to obtain the degree of Bachelor of Science
at the Delft University of Technology,
to be defended publicly on Thursday July 7, 2022 at 11:15 AM.

Student number: 4962354
Project duration: February 11, 2022 – July 7, 2022
Thesis committee: Dr. A. J. L. Adam, TU Delft, supervisor Physics
Dr. J. L. A. Dubbeldam, TU Delft, supervisor Mathematics
Dr. W. G. Bouwman, TU Delft
Dr. C. A. Urzúa Torres, TU Delft

An electronic version of this thesis is available at <http://repository.tudelft.nl/>.

Contents

Summary	iii
1 Introduction	1
2 Theory	2
2.1 Calculation of the potential	2
2.1.1 Spherical particle	3
2.1.2 Single shelled spherical particle	4
2.1.3 Janus particle	5
2.2 Calculation of force and torque	9
2.2.1 Dipole approximation	9
2.2.2 Maxwell Stress Tensor (MST)	10
2.2.3 Force and Torque derived from the Maxwell Stress Tensor	11
3 Model implementation	14
3.1 Solving for the coefficients of the potential	14
3.2 Calculating the potential with the coefficients	14
3.3 Calculation Force Maxwell Stress Tensor (MST)	14
4 Results	15
4.1 Potential calculation	15
4.1.1 Agreement with known potentials	15
4.1.2 Convergence of solution	16
4.1.3 Potential Janus particle	17
4.2 Calculation of force and torque	18
4.2.1 Dipole approximation	18
4.2.2 Maxwell Stress Tensor (MST)	18
5 Conclusion	21
A Python code	23
B Nomenclature	24
C Comparison solutions shelled particle	25
D Relative error n=1 coefficients	26

Summary

Janus particles are colloidal particles for which one half of the surface has different attributes than the other half. One property of a spherical dielectric particle with half of its surface covered by a layer of another dielectric or metal is that it has a non-uniform scattering pattern when exposed to light. However, the angle with which the light is shone on the particle has a large effect on the scattering pattern produced. Thus it is important that we are able to orient these Janus particles.

The orientation can be controlled if we apply an electric field to the particle for example. The movement of colloidal particles with an electric field is widely studied and this field is called dielectrophoresis. For a Janus particle, the calculations for the force and torque become complicated. The movement and rotation of these particles have been studied, however, no analytic solution has been found.

In this report, we derive a semi-analytic description of the force and torque due to an external electric field on a spherical Janus particle. For this, first the potential due to an external electric field is determined and then the force and torque are calculated with two methods: the dipole approximation and the Maxwell Stress Tensor method.

In the dipole approximation, there is no force on the Janus particle. But, there is a torque on the particle in the dipole approximation. Due to this torque, the Janus particle will orient itself such that its cap points in the direction perpendicular to the applied field. For the torque calculated with the Maxwell Stress Tensor, we get a similar result as in the dipole approximation. On the other hand, according to the calculations with the stress tensor, there is a relatively small force on the particle.

We recommend researching the effect that different parameters have on the agreement between the dipole approximation and the Maxwell Stress Tensor method. Furthermore, we recommend considering more complex fields for the rotation of the particle, since there is a constant force on the particle.

1

Introduction

Janus particles, named after the Roman god with two faces, are colloidal particles for which one half of the surface has different attributes (size, geometry, materials etc..) than the other half. In recent years the interest in Janus particles has grown [1] and lead to the discovery of their specific properties.

One such property is that a spherical dielectric particle with half of its surface covered by a layer of another dielectric or metal has a non-uniform scattering pattern when exposed to light [2, 3, 4]. However, the angle with which the light is shone on the particle has a large effect on the scattering pattern produced. Thus it is important that we are able to orient these Janus particles.

The orientation can be controlled if we apply an electric field to the particle for example. The movement of colloidal particles with an electric field is widely studied and this field is called dielectrophoresis [5, 6, 7]. For simpler particle geometries the force and torque can be analytically calculated. Such geometries are spheres, spheres with concentric shells [6], ellipsoids and ellipsoids with shells [8, 9]. For a Janus particle, those calculations become more complicated. The movement and rotation of Janus particles have been studied, however, no analytic solution has been found.

Chen and Jiang (2016) [10] for example experimentally observe the rotation of a Janus particle, but they approximate the Claussius-Mossotti factor of the Janus particle as the average of the factors of the shell and the core. On the other hand, Behdani *et al.* (2021) [11] draw up the full system of equations to find the electric polarizability of the particle but solve it numerically using a FEM Tool such as COMSOL.

The aim of this report is to derive a semi-analytic description of the force and torque due to an external electric field on a spherical Janus particle. We will do this by first finding the potential due to the external field. For this we need to solve the Laplace equation for the Janus particle. Then, we will calculate the force and torque with two methods: the dipole approximation and the Maxwell Stress Tensor method. We implement the calculations and perform the visualizations of the solutions in Python.

The report has the following structure: In chapter 2 we show the calculations to solve the Laplace equation and we present the calculations for the force and torque. We treat how the mathematical model is implemented in Python in chapter 3. The results of the model and their visualizations are shown and discussed in chapter 4. Finally, we list the key takeaways in chapter 5 along with recommendations for further research.

2

Theory

Let us consider a spherical Janus particle as shown in Fig. 2.1. It consists of a spherical core of radius a with an electric permittivity ϵ_c . On the northern hemisphere of the core lies a layer with thickness d , this is the shell and has permittivity ϵ_s . We set the coordinate system such that the cap points upwards in the z -direction. Lastly, the particle is suspended in a medium with permittivity ϵ_m .

We want to calculate the force and the torque on the Janus particle due to an external field, to determine if and how the particle will orient itself. Therefore, we first need to calculate the potential, Φ , of the Janus particle due to the external electric field \mathbf{E}_e . We first treat the simpler cases of a spherical particle and a spherical particle with a full shell. After that, we will calculate the potential of the Janus particle.

With the potential known, we can calculate the force and torque on the particle in two ways. First, we can compute them using the dipole approximation [7]. That is to identify the effective dipole moment, \mathbf{p}_{eff} , from the expression of the potential outside the particle. We can then calculate the force \mathbf{F} and the torque $\boldsymbol{\tau}$, with rotation point as the center of the core, with the following formulas

$$\mathbf{F} = (\mathbf{p}_{eff} \cdot \nabla) \mathbf{E}_e \quad (2.1)$$

$$\boldsymbol{\tau} = \mathbf{p}_{eff} \times \mathbf{E}_e, \quad (2.2)$$

where ∇ is the differential operator, $\nabla = (\partial/\partial x, \partial/\partial y, \partial/\partial z)$.

Second, we calculate the force and the torque using the Maxwell Stress Tensor method [12]. In this method, the Maxwell Stress Tensor $\vec{\mathbf{T}}$ is integrated over the surface of the particle. The time-averaged force and torque are thus given by

$$\langle \mathbf{F} \rangle = \oint (\vec{\mathbf{T}} \cdot \hat{\mathbf{n}}) dA \quad (2.3)$$

$$\langle \boldsymbol{\tau} \rangle = \oint r \hat{\mathbf{r}} \times (\vec{\mathbf{T}} \cdot \hat{\mathbf{n}}) dA, \quad (2.4)$$

where $\hat{\mathbf{n}}$ is the unit vector normal to the surface, r is the radial distance to the rotation point and $\hat{\mathbf{r}}$ is the radial unit vector.

2.1. Calculation of the potential

Due to the partial spherical symmetry of the systems, we use spherical coordinates (r, θ, φ) to calculate the potential. We define r as the radial distance, θ as the polar angle, $0 \leq \theta \leq \pi$, and φ as the azimuthal angle, $0 \leq \varphi < 2\pi$ as shown in Figure 2.1.

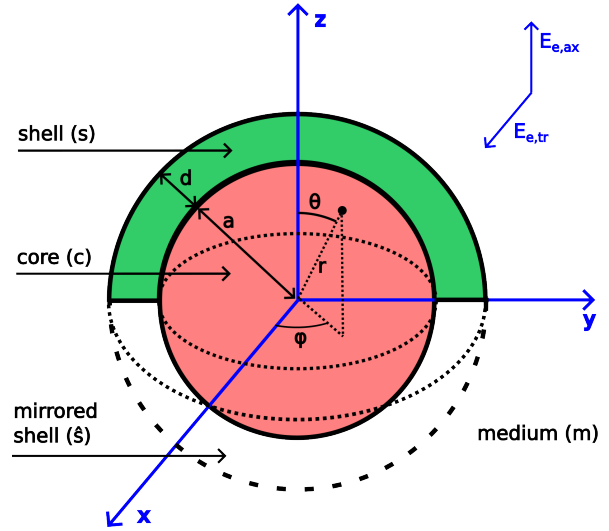


Figure 2.1: Depiction of the model of the Janus particle. The semi-shell is placed on the Northern Hemisphere.

An electrostatic potential, Φ , satisfies the Laplace equation everywhere due to the divergence- and curl-free properties of an electrostatic field. Therefore, Φ must satisfy

$$\nabla^2 \Phi = 0. \quad (2.5)$$

In the case that there is azimuthal symmetry, the solutions to the Laplace equation in spherical coordinates are well known, they are of the form [13]

$$\Phi(r, \theta) = \sum_{n=0}^{\infty} (A_n r^n + B_n r^{-(n+1)}) P_n(\xi), \quad (2.6)$$

where A_n and B_n are constants which need to be determined, P_n is the n -th order Legendre polynomial and we introduce the notation $\xi = \cos \theta$. Because of the azimuthal symmetry, the solution does not depend on φ .

2.1.1. Spherical particle

We first consider the simplest case of a dielectric spherical particle. The sphere has radius a and is centred around the origin and it has dielectric permittivity ϵ_c . It is suspended in a medium with dielectric permittivity ϵ_m . We apply an external uniform electric field \mathbf{E}_e across the particle. Without loss of generality we can assume that the electric field is oriented in the z -direction, $\mathbf{E}_e = E_e \hat{z}$. The spherical particle is shown in Figure 2.2a. The potential corresponding to this field pointing in the z -direction can be written as:

$$\Phi_e = -E_e z = -E_e r \cos \theta = -E_e r P_1(\xi), \quad (2.7)$$

with $P_1(\xi) = \xi = \cos(\theta)$ the first order Legendre polynomial. For the spherical particle, we assume that the solutions inside Φ_c and outside Φ_m the sphere are of the form:

$$\Phi_m = \Phi_e + B \frac{P_1(\xi)}{r^2} = -E_e r \cos \theta + B \frac{\cos \theta}{r^2} \quad r > a, \quad (2.8a)$$

$$\Phi_c = Ar P_1(\xi) = Ar \cos \theta \quad r < a. \quad (2.8b)$$

with A and B two constants. For $r \rightarrow \infty$ the outside solution corresponds with the potential of the applied field and at $r = 0$ the inside solution is bounded.

To find the solution we need to use the boundary conditions to solve for the coefficients A and B . There are two boundary conditions at the boundary $r = a$. First, the potential needs to be continuous.

$$\Phi_m = \Phi_c, \quad r = a, \quad \forall \theta. \quad (2.9)$$

Second, the normal component of the displacement field, $\mathbf{D} = \epsilon \mathbf{E}$, must be continuous.

$$\epsilon_m E_{m,r} = \epsilon_c E_{c,r} \Rightarrow \epsilon_m \frac{\partial \Phi_m}{\partial r} = \epsilon_c \frac{\partial \Phi_c}{\partial r}, \quad r = a, \quad \forall \theta. \quad (2.10)$$

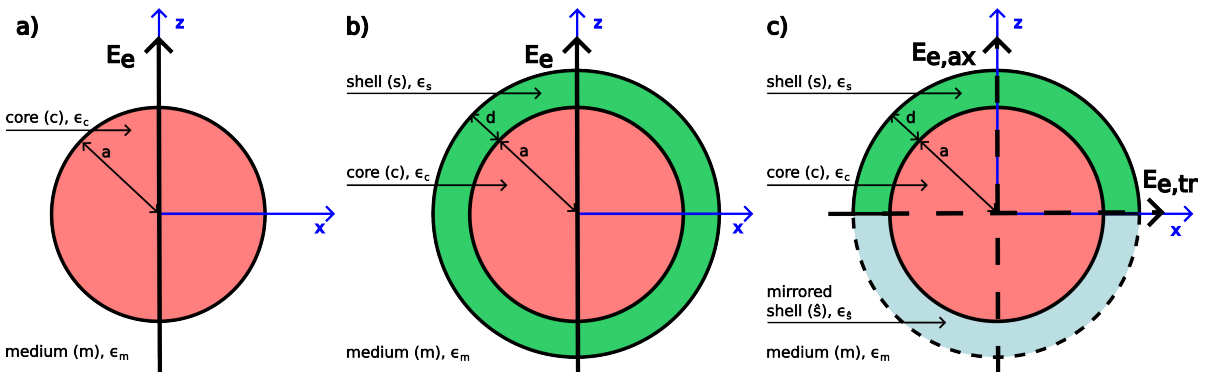


Figure 2.2: An overview of the cases we consider in section 2.1. First we consider a sphere (a), then a sphere with a concentric shell (b) and finally the Janus particle (c).

Combining Equations 2.8 with Equations 2.9 and 2.10 we get the following solutions [6]:

$$A = -\frac{3\epsilon_m}{\epsilon_c + 2\epsilon_m} E_e, \quad (2.11a)$$

$$B = \frac{\epsilon_c - \epsilon_m}{\epsilon_c + 2\epsilon_m} a^3 E_e. \quad (2.11b)$$

The fraction in Equation 2.11b is called the Clausius–Mossotti factor K_{CM} .

2.1.2. Single shelled spherical particle

The next model we consider is that of a spherical particle, with radius a , with a concentric shell around it with thickness d . The core of the particle has electric permittivity ϵ_c , the shell of the particle has ϵ_s and the medium has permittivity ϵ_m . In this case, we can also assume to have an external field \mathbf{E}_e pointing in the z -direction, $\mathbf{E}_e = E_e \hat{z}$. The single shelled sphere is depicted in Figure 2.2b.

We assume that the solutions are of the following form:

$$\Phi_m = -E_e r \cos\theta + B \frac{\cos\theta}{r^2} \quad r > a + d, \quad (2.12a)$$

$$\Phi_s = Cr \cos\theta + D \frac{\cos\theta}{r^2} \quad a < r < a + d, \quad (2.12b)$$

$$\Phi_c = Ar \cos\theta \quad r < a. \quad (2.12c)$$

with A, B, C, D being four constants to determine. We again have that at $r \rightarrow \infty$ the solution corresponds to the external potential and the solution is bounded at $r = 0$. The boundary conditions as in Equations 2.9 and 2.10 apply for the boundaries: $r = a$ and $r = a + d$, which gives us

$$r = a, \forall\theta: \begin{cases} \Phi_s = \Phi_c \\ \epsilon_s \frac{\partial\Phi_s}{\partial r} = \epsilon_c \frac{\partial\Phi_c}{\partial r}, \end{cases} \quad (2.13a)$$

$$r = a + d, \forall\theta: \begin{cases} \Phi_s = \Phi_m \\ \epsilon_s \frac{\partial\Phi_s}{\partial r} = \epsilon_m \frac{\partial\Phi_m}{\partial r}. \end{cases} \quad (2.13b)$$

If we put Equations 2.12 into the boundary conditions we get a system of 4 equations which need to be solved. In the literature, we can find two solutions to this problem. Jones (1995) [6] gives the following solution:

$$A_J = -\frac{3\epsilon_m(1-K)\zeta^3}{(\epsilon'_s + 2\epsilon_m)(\zeta^3 - K)} E_e, \quad (2.14a)$$

$$B_J = \frac{\epsilon'_s - \epsilon_m}{\epsilon'_s + 2\epsilon_m} (a + d)^3 E_e, \quad (2.14b)$$

$$C_J = -\frac{3\epsilon_m\zeta^3}{(\epsilon'_s + 2\epsilon_m)(\zeta^3 - K)} E_e, \quad (2.14c)$$

$$D_J = \frac{3\epsilon_m K (a + d)^3}{(\epsilon'_s + 2\epsilon_m)(\zeta^3 - K)} E_e, \quad (2.14d)$$

where $\zeta = (a + d)/a = 1 + d/a$, $K = (\epsilon'_s - \epsilon_m)/(\epsilon'_s + 2\epsilon_m)$ and

$$\epsilon'_s = \epsilon_s \frac{\zeta^3 + 2\left(\frac{\epsilon_c - \epsilon_s}{\epsilon_c + 2\epsilon_s}\right)}{\zeta^3 - \left(\frac{\epsilon_c - \epsilon_s}{\epsilon_c + 2\epsilon_s}\right)}. \quad (2.15)$$

Here ϵ'_s is introduced to simplify the expressions and to put Equation 2.14b in the same form as Equation 2.11b, to form a different Clausius–Mossotti factor. We can see that the potential outside of a single shelled sphere is equivalent to the potential outside of a sphere with permittivity ϵ'_s and radius $a + d$.

However, Turcu *et al.* (1989) [14] find the following coefficients:

$$A_T = -\frac{3\epsilon_m\epsilon_s}{\epsilon_s(\epsilon_c + 2\epsilon_m) + 2\mathcal{R}(\epsilon_m - \epsilon_s)(\epsilon_c - \epsilon_s)} E_e, \quad (2.16a)$$

$$B_T = \frac{\epsilon_s(\epsilon_c - \epsilon_m) - \mathcal{R}(\epsilon_m - \epsilon_s)(\epsilon_c - \epsilon_s)}{\epsilon_s(\epsilon_c + 2\epsilon_m) + 2\mathcal{R}(\epsilon_m - \epsilon_s)(\epsilon_c - \epsilon_s)} (a+d)^3 E_e, \quad (2.16b)$$

$$C_T = -\frac{\epsilon_m(\epsilon_c + 2\epsilon_s)}{\epsilon_s(\epsilon_c + 2\epsilon_m) + 2\mathcal{R}(\epsilon_m - \epsilon_s)(\epsilon_c - \epsilon_s)} E_e, \quad (2.16c)$$

$$D_T = \frac{\epsilon_m(\epsilon_c - \epsilon_s)}{\epsilon_s(\epsilon_c + 2\epsilon_m) + 2\mathcal{R}(\epsilon_m - \epsilon_s)(\epsilon_c - \epsilon_s)} a^3 E_e, \quad (2.16d)$$

where $\mathcal{R} = \frac{1}{3}[1 - \zeta^{-3}]$ was introduced.

Remarkably, these coefficients are not equal to each other. To verify which of these solutions is the correct solution we can solve the system of equations using Maple. Maple gives the following solutions:

$$A_M = \frac{9\epsilon_m\epsilon_s(a+d)^3}{(2(\zeta^{-3}-1)\epsilon_s^2 + (-2\zeta^{-3}-1)\epsilon_c + 2(-\zeta^{-3}-2)\epsilon_m)\epsilon_s + 2(\zeta^{-3}-1)\epsilon_m\epsilon_c} E_e = A_T \quad (2.17a)$$

$$B_M = \frac{(-2\zeta^{-3}+2)\epsilon_s^2 + ((\epsilon_c - 2\epsilon_m) + 2(\epsilon_c - \epsilon_m/2)\zeta^{-3})\epsilon_s + \zeta^{-3}\epsilon_c\epsilon_m - \epsilon_c\epsilon_m}{(2(\zeta^{-3}-1)\epsilon_s^2 + (-2\zeta^{-3}-1)\epsilon_c + 2(-\zeta^{-3}-2)\epsilon_m)\epsilon_s + 2(\zeta^{-3}-1)\epsilon_m\epsilon_c} (a+d)^6 E_e = B_J \quad (2.17b)$$

$$C_M = -\frac{3(\epsilon_c + 2\epsilon_s)\epsilon_m(a+d)^3}{(2(\zeta^{-3}-1)\epsilon_s^2 + (-2\zeta^{-3}-1)\epsilon_c + 2(-\zeta^{-3}-2)\epsilon_m)\epsilon_s + 2(\zeta^{-3}-1)\epsilon_m\epsilon_c} E_e = C_T \quad (2.17c)$$

$$D_M = \frac{3\epsilon_m(\epsilon_c - \epsilon_s)(a+d)^3}{(2(\zeta^{-3}-1)\epsilon_s^2 + (-2\zeta^{-3}-1)\epsilon_c + 2(-\zeta^{-3}-2)\epsilon_m)\epsilon_s + 2(\zeta^{-3}-1)\epsilon_m\epsilon_c} a^3 E_e = D_T \quad (2.17d)$$

Surprisingly, the A , C and D coefficients of the Maple solution are equal to the A , C and D coefficients of the solution given by Turcu *et al.* (1989), but the B coefficient is equal to the B coefficient given by Jones (1995). In appendix C we look at the values of the potential and the displacement field to verify which solution is correct. We will then compare the correct solution with the solution of our model to check the validity of our model.

2.1.3. Janus particle

We now consider a Janus particle as shown in Figure 2.2c in 2D and in Figure 2.1 in 3D. Since the Janus particle is not completely spherically symmetric, we can not assume that the field is only pointing in the z -direction. Due to the principle of superposition we can, however, decompose the external field, \mathbf{E}_e , into a field-oriented along the z -direction, the axial direction, and into a field-oriented perpendicular to the z -direction, the transverse direction. Without loss of generality, we can assume that the transverse direction is pointing into the x -direction.

Following the approach developed by Scherbak *et al.* (2015) [15], we mirror the shell of the particle to the southern hemisphere, to create a second half-shell. The second half-shell is visualized in Figure 2.2c as the dotted shell indicated by "mirrored shell". This second half-shell has permittivity ϵ_s . If we take the permittivity of the lower shell, ϵ_s , equal to the permittivity of the medium, ϵ_m , we will get a solution equal to the solution of a Janus particle. We first consider the case of the external field oriented along the z -direction and after that we consider the external field in the x -direction.

Janus particle in an axially oriented electric field

The potential function for each region we are considering can be written as

$$\Phi_m = \sum_{n=0}^{\infty} B_n r^{-(n+1)} P_n(\xi) - E_e r P_1(\xi) \quad r > a+d, \quad (2.18a)$$

$$\Phi_s = \sum_{n=0}^{\infty} [C_n r^n + D_n r^{-(n+1)}] P_n(\xi) \quad a \leq r \leq a+d, \quad 0 \leq \theta \leq \frac{\pi}{2}, \quad (2.18b)$$

$$\Phi_{\hat{s}} = \sum_{n=0}^{\infty} [\hat{C}_n r^n + \hat{D}_n r^{-(n+1)}] P_n(\xi) \quad a \leq r \leq a+d, \quad \frac{\pi}{2} < \theta \leq \pi, \quad (2.18c)$$

$$\Phi_c = \sum_{n=0}^{\infty} A_n r^n P_n(\xi) \quad r < a. \quad (2.18d)$$

To find the potential we need to use the boundary conditions to solve for the different coefficients (A_n , B_n , C_n , D_n , \hat{C}_n and \hat{D}_n). We require that the potential, Equation 2.9, and the displacement field, Equation 2.10, are continuous at the boundaries. Thus, we get the following boundary equations:

$$a \leq r \leq a + d, \theta = \pi/2 : \begin{cases} \Phi_s = \Phi_{\hat{s}} \\ \epsilon_s \frac{\partial \Phi_s}{\partial \theta} = \epsilon_{\hat{s}} \frac{\partial \Phi_{\hat{s}}}{\partial \theta}, \end{cases} \quad (2.19a)$$

$$r = a, 0 \leq \theta < \pi/2 : \begin{cases} \Phi_s = \Phi_c \\ \epsilon_s \frac{\partial \Phi_s}{\partial r} = \epsilon_c \frac{\partial \Phi_c}{\partial r}, \end{cases} \quad r = a, \pi/2 \leq \theta \leq \pi : \begin{cases} \Phi_{\hat{s}} = \Phi_c \\ \epsilon_{\hat{s}} \frac{\partial \Phi_{\hat{s}}}{\partial r} = \epsilon_c \frac{\partial \Phi_c}{\partial r}, \end{cases} \quad (2.19b)$$

$$r = a + d, 0 \leq \theta < \pi/2 : \begin{cases} \Phi_s = \Phi_m \\ \epsilon_s \frac{\partial \Phi_s}{\partial r} = \epsilon_m \frac{\partial \Phi_m}{\partial r}, \end{cases} \quad r = a + d, \pi/2 \leq \theta \leq \pi : \begin{cases} \Phi_{\hat{s}} = \Phi_m \\ \epsilon_{\hat{s}} \frac{\partial \Phi_{\hat{s}}}{\partial r} = \epsilon_m \frac{\partial \Phi_m}{\partial r}. \end{cases} \quad (2.19c)$$

First we solve the boundary condition in Equation 2.19a. We do this using the property of the Legendre polynomials that for n odd we have $P_n(0) = 0$ and that for n even we have $(d/d\theta)P_n(0) = 0$. Putting this into Equation 2.19a we get:

$$\hat{C}_n = \eta_n C_n, \quad (2.20a)$$

$$\hat{D}_n = \eta_n D_n, \quad (2.20b)$$

with

$$\eta_n = \begin{cases} 1 & \text{if } n \text{ even} \\ \epsilon_s / \epsilon_{\hat{s}} & \text{if } n \text{ odd.} \end{cases} \quad (2.21)$$

We now introduce the dimensionless variable $\rho = r/a$ and coefficients: $\alpha_n = A_n a^{n-1} / E_e$, $\beta_n = B_n a^{-(n+2)} / E_e$, $\gamma_n = C_n a^{n-1} / E_e$ and $\delta_n = D_n a^{-(n+2)} / E_e$ to get the following set of equations

$$\Phi_m = E_e a \left[\sum_{n=0}^{\infty} \beta_n \rho^{-(n+1)} P_n(\xi) - \rho P_1(\xi) \right], \quad (2.22a)$$

$$\Phi_s = E_e a \sum_{n=0}^{\infty} [\gamma_n \rho^n + \delta_n \rho^{-(n+1)}] P_n(\xi), \quad (2.22b)$$

$$\Phi_{\hat{s}} = E_e a \sum_{n=0}^{\infty} [\gamma_n \rho^n + \delta_n \rho^{-(n+1)}] \eta_n P_n(\xi), \quad (2.22c)$$

$$\Phi_c = E_e a \sum_{n=0}^{\infty} \alpha_n \rho^n P_n(\xi). \quad (2.22d)$$

To solve for the coefficients α_n , β_n , γ_n and δ_n we insert Equations 2.22 into their respective boundary conditions in Equations 2.19b and Equations 2.19c. We get the following system of equations; where we use that for $r = a$ we have $\rho = 1$ and that for $r = a + d$ we have $\rho = 1 + d/a = \zeta$. For $r = a$ we have

$$\sum_{n=0}^{\infty} [\gamma_n + \delta_n] \eta_n^{(s,\hat{s})} P_n(\xi) = \sum_{n=0}^{\infty} \alpha_n P_n(\xi), \quad (2.23)$$

$$\sum_{n=0}^{\infty} [n\gamma_n - (n+1)\delta_n] \epsilon_{s,\hat{s}} \eta_n^{(s,\hat{s})} P_n(\xi) = \sum_{n=0}^{\infty} n\alpha_n \epsilon_c P_n(\xi). \quad (2.24)$$

Here we write the equations compactly by introducing the sub- and superscripts s and \hat{s} . We retrieve the equation for $0 \leq \xi \leq 1$ by taking s in the sub- and superscripts, where we have that $\eta_n^{(s)} = 1$. The equation for $-1 \leq \xi \leq 0$ is obtained by taking \hat{s} in the sub- and superscripts and $\eta_n^{(\hat{s})}$ is the same η_n as in Equation 2.21.

Similarly, with the same notation, we have for the boundary at $r = a + d$

$$\sum_{n=0}^{\infty} [\zeta^{n-1} \gamma_n + \zeta^{-(n+2)} \delta_n] \eta_n^{(s,\hat{s})} P_n(\xi) = \sum_{n=0}^{\infty} \zeta^{-(n+2)} \beta_n P_n(\xi) - P_1(\xi) \quad (2.25)$$

$$\sum_{n=0}^{\infty} [n\zeta^{n-1} \gamma_n - (n+1)\zeta^{-(n+2)} \delta_n] \epsilon_{s,\hat{s}} \eta_n^{(s,\hat{s})} P_n(\xi) = \sum_{n=0}^{\infty} -(n+1)\zeta^{-(n+2)} \beta_n \epsilon_m P_n(\xi) - \epsilon_m P_1(\xi). \quad (2.26)$$

Solving for the coefficients now becomes more difficult, since the Legendre polynomials do not form a complete set on $0 \leq \xi \leq 1$ or $-1 \leq \xi \leq 0$.

To solve this problem and to create a system of equations, we cut-off the sums in each equation at N . We then multiply each equation by $P_k(\xi)$, for different values of k ranging from $k = 0$ to $k = N$. If we do this to the Equations in 2.23, we get

$$\sum_{n=0}^N [\gamma_n + \delta_n] P_k(\xi) P_n(\xi) = \sum_{n=0}^N \alpha_n P_k(\xi) P_n(\xi) \quad 0 < \xi \leq 1, \quad 0 \leq k \leq N, \quad (2.27)$$

$$\sum_{n=0}^N [\gamma_n + \delta_n] \eta_n P_k(\xi) P_n(\xi) = \sum_{n=0}^N \alpha_n P_k(\xi) P_n(\xi) \quad -1 \leq \xi < 0, \quad 0 \leq k \leq N. \quad (2.28)$$

Then we integrate over the respective domain of each equation, $0 \leq \xi \leq 1$ for index s and $-1 \leq \xi \leq 0$ for index \hat{s} . Now we can add the equations of index \hat{s} to their corresponding equations of index s . Thus by adding Equation 2.28 to Equation 2.27 we obtain

$$\begin{aligned} \sum_{n=0}^N [\gamma_n + \delta_n] \left[\int_0^1 P_k(\xi) P_n(\xi) d\xi + \eta_n \int_{-1}^0 P_k(\xi) P_n(\xi) d\xi \right] = \\ = \sum_{n=0}^N \alpha_n \left[\int_0^1 P_k(\xi) P_n(\xi) d\xi + \int_{-1}^0 P_k(\xi) P_n(\xi) d\xi \right] \quad 0 \leq k \leq N. \end{aligned} \quad (2.29)$$

If we use the property that the P_n is an even function for even n and P_n is odd for odd n , $P_n(-x) = (-1)^n P_n(x)$, we get the following

$$\int_{-1}^0 P_n(\xi) P_k(\xi) d\xi = (-1)^{n+k} \int_0^1 P_n(\xi) P_k(\xi) d\xi. \quad (2.30)$$

We can use this to rewrite Equation 2.29.

$$\sum_{n=0}^N [\gamma_n + \delta_n] \left[1 + \eta_n (-1)^{n+k} \right] U_{n,k} = \sum_{n=0}^N \alpha_n \left[1 + (-1)^{n+k} \right] U_{n,k} \quad 0 \leq k \leq N, \quad (2.31)$$

where we introduce the notation $U_{n,k} = \int_0^1 P_n(\xi) P_k(\xi) d\xi$. These integrals are computed analytically by Kettunen *et al.* (2007) [16]. If we also do these steps for Equations 2.24, 2.25 and 2.26, we obtain a system of $4(N+1)$ equations, which we can write in matrix form:

$$\begin{bmatrix} A_1 & B_1 & C_1 & D_1 \\ A_2 & B_2 & C_2 & D_2 \\ A_3 & B_3 & C_3 & D_3 \\ A_4 & B_4 & C_4 & D_4 \end{bmatrix} \begin{bmatrix} \boldsymbol{\alpha} \\ \boldsymbol{\beta} \\ \boldsymbol{\gamma} \\ \boldsymbol{\delta} \end{bmatrix} = \begin{bmatrix} R_1 \\ R_2 \\ R_3 \\ R_4 \end{bmatrix}, \quad (2.32)$$

where $\boldsymbol{\alpha}$, $\boldsymbol{\beta}$, $\boldsymbol{\gamma}$ and $\boldsymbol{\delta}$ are vectors of length $N+1$ and contain the coefficients for which we want to solve. The matrix, M , and the vector, \mathbf{R} , on the right can be written as:

$$\begin{aligned}
A_1^{kn} &= -\left[1 + (-1)^{n+k}\right] U_{n,k} & B_1^{kn} &= 0 \\
A_2^{kn} &= -\left[1 + (-1)^{n+k}\right] n\epsilon_c U_{n,k} & B_2^{kn} &= 0 \\
A_3^{kn} &= 0 & B_3^{kn} &= -\left[1 + (-1)^{n+k}\right] \zeta^{-(n+2)} U_{n,k} \\
A_4^{kn} &= 0 & B_4^{kn} &= \left[1 + (-1)^{n+k}\right] (n+1)\epsilon_m \zeta^{-(n+2)} U_{n,k} \\
\\
C_1^{kn} &= \left[1 + \eta_n (-1)^{n+k}\right] U_{n,k} & D_1^{kn} &= \left[1 + \eta_n (-1)^{n+k}\right] U_{n,k} \\
C_2^{kn} &= \left[\epsilon_{s1} + \epsilon_{s2} \eta_n (-1)^{n+k}\right] n U_{n,k} & D_2^{kn} &= -\left[\epsilon_{s1} + \epsilon_{s2} \eta_n (-1)^{n+k}\right] (n+1) U_{n,k} \\
C_3^{kn} &= \left[1 + \eta_n (-1)^{n+k}\right] \zeta^{n-1} U_{n,k} & D_3^{kn} &= \left[1 + \eta_n (-1)^{n+k}\right] \zeta^{-(n+2)} U_{n,k} \\
C_4^{kn} &= \left[\epsilon_{s1} + \epsilon_{s2} \eta_n (-1)^{n+k}\right] n \zeta^{n-1} U_{n,k} & D_4^{kn} &= -\left[\epsilon_{s1} + \epsilon_{s2} \eta_n (-1)^{n+k}\right] (n+1) \zeta^{-(n+2)} U_{n,k}
\end{aligned} \tag{2.33}$$

$$\begin{aligned}
R_1^k &= 0 \\
R_2^k &= 0 \\
R_3^k &= -\left[1 - (-1)^k\right] U_{1,k} \\
R_4^k &= -\left[1 - (-1)^k\right] \epsilon_m U_{1,k}.
\end{aligned}$$

This system of equations can not be solved analytically [15], thus we solve this system numerically to get the desired coefficients. Finally, we obtain the coefficients \hat{C}_n and \hat{D}_n with the relation in Equation 2.20.

Janus particle in a transverse oriented electric field

If we have a field pointing in the x -direction we lose our azimuthal symmetry, so we cannot describe the potential with Legendre polynomials. But, we can describe them with associated Legendre polynomials P_n^m multiplied by $\cos m\varphi$. For this report, we use the associated Legendre polynomials without the Condon-Shortley phase. We can write the potential as:

$$\Phi_e = -E_e x = -E_e r \sin\theta \cos\varphi = -E_e r P_1^1(\xi) \cos\varphi. \tag{2.34}$$

Now the potentials which are expanded in associated Legendre polynomials with a $\cos\varphi$ dependency are of the form [16]:

$$\Phi_m = \sum_{n=1}^{\infty} B_n r^{-(n+1)} P_n^1(\xi) \cos\varphi - E_e r P_1^1(\xi) \cos\varphi \quad r > a + d, \tag{2.35a}$$

$$\Phi_s = \sum_{n=1}^{\infty} [C_n r^n + D_n r^{-(n+1)}] P_n^1(\xi) \cos\varphi \quad a \leq r \leq a + d, \quad 0 \leq \theta \leq \frac{\pi}{2}, \tag{2.35b}$$

$$\Phi_{\delta} = \sum_{n=1}^{\infty} [\hat{C}_n r^n + \hat{D}_n r^{-(n+1)}] P_n^1(\xi) \cos\varphi \quad a \leq r \leq a + d, \quad \frac{\pi}{2} < \theta \leq \pi, \tag{2.35c}$$

$$\Phi_c = \sum_{n=1}^{\infty} A_n r^n P_n^1(\xi) \cos\varphi \quad r < a. \tag{2.35d}$$

To solve for the coefficients we have the same boundary conditions as for the field oriented in the z -direction (Equations 2.19), where the conditions must also hold for all φ . Again we first solve the boundary condition between the two semi-shells. This is done using the property that for the associated Legendre polynomials we have even values of n , $P_n^1(0) = 0$ and for odd values of n , $\partial P_n^1 / \partial \theta(0) = 0$. Putting this into Equation 2.19a we obtain

$$\hat{C}_n = \eta'_n C_n, \tag{2.36a}$$

$$\hat{D}_n = \eta'_n D_n, \tag{2.36b}$$

with

$$\eta'_n = \begin{cases} 1 & \text{if } n \text{ even} \\ \epsilon_s/\epsilon_\delta & \text{if } n \text{ odd.} \end{cases} \quad (2.37)$$

To obtain the other coefficients we use the same approach as in the axial case, however we multiply each equation with $P_k^1(\xi)$ for different values of k from $k = 1$ to $k = N$. Then we integrate over the domain of each equation and use the property that $P_n^m(-x) = (-1)^{n+m} P_n^m(x)$ to rewrite $\int_{-1}^0 P_n^1(\xi) P_k^1(\xi) d\xi = (-1)^{n+k} \int_0^1 P_n^1(\xi) P_k^1(\xi) d\xi$. We eventually get the same system of equations as in Equation 2.33 only with η_n replaced by η'_n and $U_{n,k}$ replaced by $U_{n,k}^1 = \int_0^1 P_n^1(\xi) P_k^1(\xi) d\xi$. These integrals are also computed analytically by Kettunen *et al.* (2007) [16]. The system of equations again needs to be solved numerically and we obtain the final coefficients \hat{C}_n and \hat{D}_n with Equation 2.36.

2.2. Calculation of force and torque

We now have defined the potential everywhere. With this information we can calculate the force and torque on the Janus particle. We use two methods for the calculations. First we use the dipole approximation, this method reduces the particle to the simpler model of a dipole and these calculations can be done analytically. Second we use the Maxwell Stress Tensor method, this method is the most rigorous approach to calculate the force and torque [6], however the calculations have to be done numerically.

2.2.1. Dipole approximation

In an electric field, the particle becomes polarized and creates a secondary electric field. This induced field can be approximated by the field of a dipole. The polarizability χ is a parameter which describes the magnitude of the polarization and is defined as the ratio between the effective dipole moment and the magnitude of the electric field.

$$\mathbf{p}_{eff} = \chi \mathbf{E}_e. \quad (2.38)$$

To determine the polarizability χ we have to consider the potential of a dipole and compare it with the dipolar term ($n = 1$) of the series expansion in Equations 2.18a or 2.35a.

The potential of an electric dipole, which is z -directed, is of the form [6]

$$\Phi_d = \frac{p_{eff} \cos \theta}{4\pi\epsilon_m r^2}. \quad (2.39)$$

The dipolar term of the series expansion of the axial case is

$$\Phi_{d,ax} = \frac{B_1 P_1(\xi)}{r^2} = \frac{B_1 \cos \theta}{r^2}. \quad (2.40)$$

Thus we have for the polarizability

$$p_{eff,ax} = 4\pi\epsilon_m B_{1,ax} = 4\pi\epsilon_m a^3 E_e \beta_{1,ax} = \chi_{ax} E_e, \quad (2.41)$$

$$p_{eff,tr} = 4\pi\epsilon_m B_{1,tr} = 4\pi\epsilon_m a^3 E_e \beta_{1,tr} = \chi_{tr} E_e, \quad (2.42)$$

where $p_{eff,tr}$ was derived similarly as $p_{eff,ax}$, but with the expression of a x -directed dipole.

For a object with a rotational symmetry, around the z -axis, we can write it the effective dipole moment a more general form [16]:

$$\mathbf{p}_{eff} = \tilde{\chi} \cdot \mathbf{E}_e, \quad (2.43)$$

where the polarizability dyadic is of the form

$$\tilde{\chi} = \chi_{tr} (\hat{x}\hat{x} + \hat{y}\hat{y}) + \chi_{ax} \hat{z}\hat{z}. \quad (2.44)$$

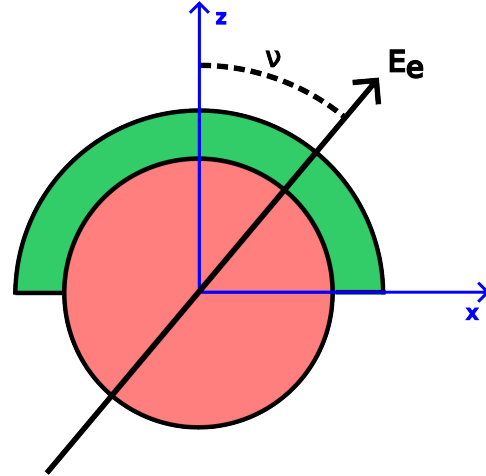


Figure 2.3: Depiction Janus particle with the field incident with the angle ν .

We define the angle ν as the angle between the z-axis and the field, as shown in Figure 2.3. Then we can represent the field as:

$$\mathbf{E}_e = [\sin \nu \hat{\mathbf{x}} + \cos \nu \hat{\mathbf{z}}] E_e. \quad (2.45)$$

Now we can write the effective dipole moment of the particle as

$$\mathbf{p}_{eff} = [\chi_{tr} \sin \nu \hat{\mathbf{x}} + \chi_{tr} \cos \nu \hat{\mathbf{z}}] E_e. \quad (2.46)$$

Since the field is uniform there is no force on the Janus particle as stated by Equation 2.1. Using Equation 2.2 we can calculate that the torque on the particle is

$$\boldsymbol{\tau} = [\chi_{ax} - \chi_{tr}] \frac{E_e^2}{2} \sin 2\nu \hat{\mathbf{y}}. \quad (2.47)$$

From this equation, we can see that depending on the difference between the axial and the transverse polarizability one of $\nu = 0$ or $\nu = \pi/2$ is a stable equilibrium and the other is an unstable equilibrium.

2.2.2. Maxwell Stress Tensor (MST)

In order to compute the force and torque in a different way, we introduce the Maxwell Stress Tensor. This is defined for any electric field \mathbf{E} as [12]

$$\vec{\mathbf{T}} = \epsilon \left(\mathbf{E}\mathbf{E} - \frac{1}{2} |\mathbf{E}|^2 \vec{\mathbf{I}} \right) \quad (2.48)$$

where $\vec{\mathbf{I}}$ is the unit tensor and the product of two vectors without a dot denotes the dyadic product.

Before we can calculate the stress tensor we first have to calculate the electric field from the potential. For spherical coordinates, we have the following formula to calculate the electric field

$$\mathbf{E} = -\nabla\Phi = -\frac{\partial\Phi}{\partial r} \hat{\mathbf{r}} - \frac{1}{r} \frac{\partial\Phi}{\partial\theta} \hat{\boldsymbol{\theta}} - \frac{1}{r \sin\theta} \frac{\partial\Phi}{\partial\varphi} \hat{\boldsymbol{\phi}}. \quad (2.49)$$

We determine the field attached to the potential in its general form, Equation 2.6 and then we can use the coefficients determined by the model for each area. So we obtain the following field in the axial case:

$$E_r^{ax} = -\sum_{n=0}^N [nA_n r^{n-1} - (n+1)B_n r^{-(n+2)}] P_n(\xi), \quad (2.50a)$$

$$E_\theta^{ax} = \sum_{n=0}^N [A_n r^{n-1} + B_n r^{-(n+2)}] \sin\theta \frac{n}{\xi^2 - 1} [\xi P_n(\xi) - P_{n-1}(\xi)], \quad (2.50b)$$

$$E_\varphi^{ax} = 0, \quad (2.50c)$$

where we used that $(x^2 - 1) \frac{dP_n}{dx} = n(xP_n(x) - P_{n-1}(x))$. The sum stops at N since we only calculated the coefficients up to N . If the external field is in the transverse direction, we get the following field as a result

$$E_r^{tr} = -\sum_{n=0}^N [nA_n r^{n-1} - (n+1)B_n r^{-(n+2)}] P_n^1(\xi) \cos\varphi, \quad (2.51a)$$

$$E_\theta^{tr} = \sum_{n=0}^N [A_n r^{n-1} + B_n r^{-(n+2)}] \sin\theta \frac{1}{\xi^2 - 1} [n\xi P_n^1(\xi) - (n+1)P_{n-1}^1(\xi)] \cos\varphi, \quad (2.51b)$$

$$E_\varphi^{tr} = \sum_{n=0}^N [A_n r^{n-1} + B_n r^{-(n+2)}] \frac{P_n^1(\xi)}{\sin\theta} \sin\varphi, \quad (2.51c)$$

where we used the property of the associated Legendre polynomials that:

$$(x^2 - 1) \frac{dP_n^m}{dx} = nxP_n^m(x) - (n+m)P_{n-1}^m(x).$$

We have now calculated the electric field in spherical coordinates. To turn this into a vector field of Cartesian coordinates we use the following relations:

$$\hat{\mathbf{r}} = \sin\theta(\cos\varphi \hat{\mathbf{x}} + \sin\varphi \hat{\mathbf{y}}) + \cos\theta \hat{\mathbf{z}}, \quad (2.52a)$$

$$\hat{\boldsymbol{\theta}} = \cos\theta(\cos\varphi \hat{\mathbf{x}} + \sin\varphi \hat{\mathbf{y}}) - \sin\theta \hat{\mathbf{z}}, \quad (2.52b)$$

$$\hat{\boldsymbol{\phi}} = -\sin\varphi \hat{\mathbf{x}} + \cos\varphi \hat{\mathbf{y}}. \quad (2.52c)$$

If we have an external field of the form as given in Equation 2.45, the resulting field will be the sum of the field caused by an external field in the axial direction and in the transverse direction.

$$\mathbf{E} = \sin \nu \mathbf{E}^{tr} + \cos \nu \mathbf{E}^{ax}. \quad (2.53)$$

If we plug this into Equation 2.48 we obtain the following:

$$\tilde{\mathbf{T}} = \epsilon \left(\sin^2 \nu \left[\mathbf{E}^{tr} \mathbf{E}^{tr} - \frac{1}{2} |\mathbf{E}^{tr}|^2 \tilde{\mathbf{I}} \right] + \cos^2 \nu \left[\mathbf{E}^{ax} \mathbf{E}^{ax} - \frac{1}{2} |\mathbf{E}^{ax}|^2 \tilde{\mathbf{I}} \right] + \sin \nu \cos \nu \left[\mathbf{E}^{tr} \mathbf{E}^{ax} + \mathbf{E}^{ax} \mathbf{E}^{tr} - \mathbf{E}^{ax} \cdot \mathbf{E}^{tr} \tilde{\mathbf{I}} \right] \right) \quad (2.54)$$

$$= \sin^2 \nu \tilde{\mathbf{T}}^{tr} + \cos^2 \nu \tilde{\mathbf{T}}^{ax} + \sin \nu \cos \nu \tilde{\mathbf{T}}^{cross} \quad (2.55)$$

The stress tensor is thus a sum of the stress tensor related to a field in the axial direction, the tensor related to a field in the transverse direction and a cross term. We get the following for each individual tensor.

$$\tilde{\mathbf{T}}^{ax} = \frac{\epsilon_m}{2} \begin{bmatrix} E_r^2 - E_\theta^2 & 2E_r E_\theta & 0 \\ 2E_r E_\theta & -E_r^2 + E_\theta^2 & 0 \\ 0 & 0 & -E_r^2 - E_\theta^2 \end{bmatrix} = \begin{bmatrix} T_{rr} & T_{r\theta} & T_{r\varphi} \\ T_{\theta r} & T_{\theta\theta} & T_{\theta\varphi} \\ T_{\varphi r} & T_{\varphi\theta} & T_{\varphi\varphi} \end{bmatrix}. \quad (2.56)$$

$$\tilde{\mathbf{T}}^{tr} = \frac{\epsilon_m}{2} \begin{bmatrix} [E_r^2 - E_\theta^2] \cos^2 \varphi - E_\varphi^2 \sin^2 \varphi & 2E_r E_\theta \cos^2 \varphi & 2E_r E_\varphi \sin \varphi \cos \varphi \\ 2E_r E_\theta \cos^2 \varphi & [-E_r^2 + E_\theta^2] \cos^2 \varphi - E_\varphi^2 \sin^2 \varphi & 2E_\theta E_\varphi \sin \varphi \cos \varphi \\ 2E_r E_\varphi \sin \varphi \cos \varphi & 2E_\theta E_\varphi \sin \varphi \cos \varphi & -[E_r^2 + E_\theta^2] \cos^2 \varphi + E_\varphi^2 \sin^2 \varphi \end{bmatrix}. \quad (2.57)$$

$$\tilde{\mathbf{T}}^{cross} = \epsilon_m \begin{bmatrix} [E_r^{ax} E_r^{tr} - E_\theta^{ax} E_\theta^{tr}] \cos \varphi & [E_\theta^{ax} E_r^{tr} + E_r^{ax} E_\theta^{tr}] \cos \varphi & E_r^{ax} E_\varphi^{tr} \sin \varphi \\ [E_\theta^{ax} E_r^{tr} + E_r^{ax} E_\theta^{tr}] \cos \varphi & [-E_r^{ax} E_r^{tr} + E_\theta^{ax} E_\theta^{tr}] \cos \varphi & E_\theta^{ax} E_\varphi^{tr} \sin \varphi \\ E_r^{ax} E_\varphi^{tr} \sin \varphi & E_\theta^{ax} E_\varphi^{tr} \sin \varphi & -[E_r^{ax} E_r^{tr} + E_\theta^{ax} E_\theta^{tr}] \cos \varphi \end{bmatrix}. \quad (2.58)$$

In Equations 2.56 and 2.57 we omit the superscript on the field components for readability. In Equation 2.56 we also introduce the general notation for each element of the tensors. In Equations 2.57 and 2.58 we take the φ dependence outside of the field components, to simplify the evaluations of the integrals later.

2.2.3. Force and Torque derived from the Maxwell Stress Tensor

The force and torque are calculated by integrating the stress tensor, calculated with the field outside of the surface, over the surface of the Janus particle. In order to make the calculation clear, we partition the Janus particle into three distinct surfaces, which are indicated in Figure 2.4.:

1. the spherical dome of the shell, $r = a + d$, $0 \leq \theta < \pi/2$ and $0 \leq \varphi < 2\pi$, its vector normal to the surface points is $\hat{\mathbf{n}}_1 = \hat{\mathbf{r}}$.

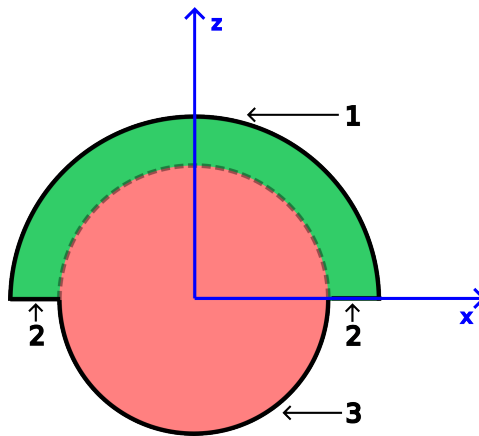


Figure 2.4: Depiction of the integration surfaces of the Janus particle. The indicated surfaces need to be revolved around the z -axis.

2. The thin ring at the bottom of the shell, $a \leq r \leq a + d$, $\theta = \pi/2$ and $0 \leq \varphi < 2\pi$. This surface has normal vector $\hat{\mathbf{n}}_2 = \hat{\boldsymbol{\theta}}$.
3. The lower hemisphere of the core, $r = a$, $\pi/2 < \theta \leq \pi$ and $0 \leq \varphi < 2\pi$, which has $\hat{\mathbf{n}}_3 = \hat{\mathbf{r}}$ as its normal vector.

Because of the linearity of the integral, the dot product and the cross product, we can calculate the torque and force independently for each component of the tensor. For example, the force due to the field in the axial case is then calculated as

$$\langle \mathbf{F}^{ax} \rangle = \oint (\vec{\mathbf{T}}^{ax} \cdot \hat{\mathbf{n}}) dA = \iint_1 (\vec{\mathbf{T}}^{ax} \cdot \hat{\mathbf{r}}) dA + \iint_2 (\vec{\mathbf{T}}^{ax} \cdot \hat{\boldsymbol{\theta}}) dA + \iint_3 (\vec{\mathbf{T}}^{ax} \cdot \hat{\mathbf{r}}) dA \quad (2.59)$$

$$= \langle \mathbf{F}_1^{ax} \rangle + \langle \mathbf{F}_2^{ax} \rangle + \langle \mathbf{F}_3^{ax} \rangle \quad (2.60)$$

Force calculations

We consider the integrals over the first and third surfaces together since they have the same normal vector.

$$\langle \mathbf{F}_{1,3} \rangle = \iint_{1,3} (\vec{\mathbf{T}} \cdot \hat{\mathbf{r}}) dA = \iint_{1,3} (T_{rr} \hat{\mathbf{r}} + T_{r\theta} \hat{\boldsymbol{\theta}} + T_{r\varphi} \hat{\boldsymbol{\phi}}) R^2 \sin \theta d\theta d\varphi. \quad (2.61)$$

$$= \iint_{1,3} (T_{rr} [\sin \theta (\cos \varphi \hat{\mathbf{x}} + \sin \varphi \hat{\mathbf{y}}) + \cos \theta \hat{\mathbf{z}}] + T_{r\theta} [\cos \theta (\cos \varphi \hat{\mathbf{x}} + \sin \varphi \hat{\mathbf{y}}) - \sin \theta \hat{\mathbf{z}}] + T_{r\varphi} [-\sin \varphi \hat{\mathbf{x}} + \cos \varphi \hat{\mathbf{y}}]) R^2 \sin \theta d\theta d\varphi. \quad (2.62)$$

Above we introduced R for which we have $R = a + d$ for surface 1 and $R = a$ for surface 3. Furthermore, we expand the unit vectors in spherical coordinates into Cartesian unit vectors with Equations 2.52. For surface 1 we need to integrate θ from $\theta = 0$ to $\theta = \pi/2$ and for surface 3 we need to integrate from $\theta = \pi/2$ to $\theta = \pi$.

For the field due to an axial external field, we do not have a φ dependence in the tensor. If we integrate over φ from $\varphi = 0$ to $\varphi = 2\pi$, we see that all the terms with $\cos \varphi$ and $\sin \varphi$ drop out. Thus we remain with the following

$$\langle \mathbf{F}_{1,3}^{ax} \rangle = \epsilon_m \pi R^2 \int_{1,3} (T_{rr} \cos \theta - T_{r\theta} \sin \theta) \sin \theta d\theta \hat{\mathbf{z}} \quad (2.63)$$

$$= \epsilon_m \pi R^2 \int_{1,3} [(E_r^2 - E_\theta^2) \cos \theta - 2E_r E_\theta \sin \theta] \sin \theta d\theta \hat{\mathbf{z}}. \quad (2.64)$$

For the field due to a transverse external field, each component of the tensor has a $\sin^2 \varphi$, $\cos^2 \varphi$ or $\sin \varphi \cos \varphi$ dependence. We know that the integrals of $\cos^3 \varphi$, $\cos^2 \varphi \sin \varphi$, $\cos \varphi \sin^2 \varphi$ and $\sin^3 \varphi$ from $\varphi = 0$ to $\varphi = 2\pi$ are all zero. Thus we can see that all the terms containing $\hat{\mathbf{x}}$ and $\hat{\mathbf{y}}$ drop out and what remains is:

$$\langle \mathbf{F}_{1,3}^{tr} \rangle = \frac{\epsilon_m \pi}{2} R^2 \int_{1,3} \left([E_r^2 - E_\theta^2 - E_\varphi^2] \cos \theta - 2E_r E_\theta \sin \theta \right) \sin \theta d\theta \hat{\mathbf{z}}, \quad (2.65)$$

where we used that $\int_0^{2\pi} \cos^2 \varphi d\varphi = \int_0^{2\pi} \sin^2 \varphi d\varphi = \pi$.

For the cross-term in the stress tensor, we see that each element of the tensor has a $\sin \varphi$ or $\cos \varphi$ dependence. Thus now the terms with $\sin \varphi$, $\cos \varphi$ and $\sin \varphi \cos \varphi$ drop out as a result of the integration over φ , which are the y - and z -components. So we remain with

$$\langle \mathbf{F}_{1,3}^{cross} \rangle = \epsilon_m \pi R^2 \int_{1,3} \left([E_r^{ax} E_r^{tr} - E_\theta^{ax} E_\theta^{tr}] \sin \theta + [E_\theta^{ax} E_r^{tr} + E_r^{ax} E_\theta^{tr}] \cos \theta - E_r^{ax} E_\varphi^{tr} \right) \sin \theta d\theta \hat{\mathbf{x}}. \quad (2.66)$$

For the second surface, we have the following

$$\langle \mathbf{F}_2 \rangle = \iint_2 (\vec{\mathbf{T}} \cdot \hat{\boldsymbol{\theta}}) dA = \iint_2 (T_{\theta r} \hat{\mathbf{r}} + T_{\theta\theta} \hat{\boldsymbol{\theta}} + T_{\theta\varphi} \hat{\boldsymbol{\phi}}) r \sin \theta dr d\varphi \quad (2.67)$$

$$= \iint_2 (T_{\theta r} [\sin \theta (\cos \varphi \hat{\mathbf{x}} + \sin \varphi \hat{\mathbf{y}}) + \cos \theta \hat{\mathbf{z}}] + T_{\theta\theta} [\cos \theta (\cos \varphi \hat{\mathbf{x}} + \sin \varphi \hat{\mathbf{y}}) - \sin \theta \hat{\mathbf{z}}] + T_{\theta\varphi} [-\sin \varphi \hat{\mathbf{x}} + \cos \varphi \hat{\mathbf{y}}]) r \sin \theta dr d\varphi. \quad (2.68)$$

Following the same steps as above for each tensor component, we get the following formulas

$$\langle \mathbf{F}_2^{ax} \rangle = \epsilon_m \pi \int_a^{a+d} [E_r^2 - E_\theta^2] r dr \hat{\mathbf{z}}, \quad (2.69)$$

$$\langle \mathbf{F}_2^{tr} \rangle = \frac{\epsilon_m \pi}{2} \int_a^{a+d} [E_r^2 - E_\theta^2 + E_\varphi^2] r dr \hat{\mathbf{z}}, \quad (2.70)$$

$$\langle \mathbf{F}_2^{cross} \rangle = \epsilon_m \pi \int_a^{a+d} [E_\theta^{ax} E_r^{tr} + E_r^{ax} E_\theta^{tr} - E_\theta^{ax} E_\varphi^{tr}] r dr \hat{\mathbf{x}}, \quad (2.71)$$

where we used that $\theta = \pi/2$. The integrals in Equations 2.64, 2.65, 2.66, 2.69, 2.70 and 2.71 are evaluated numerically. It might be possible to evaluate the integrals analytically, however, this goes beyond the scope of this report.

Finally, the expression of the total force on the particle is

$$\langle \mathbf{F} \rangle = \sin^2 \nu \langle \mathbf{F}^{tr} \rangle + \cos^2 \nu \langle \mathbf{F}^{ax} \rangle + \cos \nu \sin \nu \langle \mathbf{F}^{cross} \rangle. \quad (2.72)$$

Torque calculations

We again treat surfaces 1 and 3 together, so the formula for the torque becomes

$$\langle \boldsymbol{\tau}_{1,3} \rangle = \iint_{1,3} r \hat{\mathbf{r}} \times (\vec{\mathbf{T}} \cdot \hat{\mathbf{r}}) dA = \iint_{1,3} R \hat{\mathbf{r}} \times (T_{rr} \hat{\mathbf{r}} + T_{r\theta} \hat{\boldsymbol{\theta}} + T_{r\varphi} \hat{\boldsymbol{\varphi}}) R^2 \sin \theta d\theta d\varphi \quad (2.73)$$

$$= R^3 \iint_{1,3} (-T_{r\varphi} \hat{\boldsymbol{\theta}} + T_{r\theta} \hat{\boldsymbol{\varphi}}) \sin \theta d\theta d\varphi \quad (2.74)$$

$$= R^3 \iint_{1,3} (-T_{r\varphi} [\cos \theta (\cos \varphi \hat{\mathbf{x}} + \sin \varphi \hat{\mathbf{y}}) - \sin \theta \hat{\mathbf{z}}] + T_{r\theta} [-\sin \varphi \hat{\mathbf{x}} + \cos \varphi \hat{\mathbf{y}}]) \sin \theta d\theta d\varphi. \quad (2.75)$$

For the case of the external field pointing in the axial direction, we have that $T_{r\varphi} = 0$ and that the integral over a sine or cosine is zero. For the transverse case, $T_{r\varphi}$ has a $\cos \varphi \sin \varphi$ dependence and $T_{r\theta}$ has a $\cos^2 \varphi$ dependence. Due to this the integral from $\varphi = 0$ to $\varphi = 2\pi$ also yields zero. Thus we see that, in both cases, there is no torque contribution due to these surfaces.

$$\langle \boldsymbol{\tau}_{1,3}^{ax} \rangle = \langle \boldsymbol{\tau}_{1,3}^{tr} \rangle = 0. \quad (2.76)$$

For the cross tensor we have that $T_{r\varphi}$ has a $\sin \varphi$ dependence and $T_{r\theta}$ has a $\cos \varphi$ dependence. Hence, only the terms with $\hat{\mathbf{y}}$ remain and we get the following integral for the torque

$$\langle \boldsymbol{\tau}_{1,3}^{cross} \rangle = \epsilon_m \pi R^3 \int_{1,3} (-E_r^{ax} E_\varphi^{tr} \cos \theta + E_\theta^{ax} E_r^{tr} + E_r^{ax} E_\theta^{tr}) \sin \theta d\theta \hat{\mathbf{y}}. \quad (2.77)$$

For the second surface we get the following formula for the torque

$$\langle \boldsymbol{\tau}_2 \rangle = \iint_2 r \hat{\mathbf{r}} \times (\vec{\mathbf{T}} \cdot \hat{\boldsymbol{\theta}}) dA = \iint_2 r \hat{\mathbf{r}} \times (T_{\theta r} \hat{\mathbf{r}} + T_{\theta\theta} \hat{\boldsymbol{\theta}} + T_{\theta\varphi} \hat{\boldsymbol{\varphi}}) r \sin \theta dr d\varphi \quad (2.78)$$

$$= \iint_2 (-T_{\theta\varphi} \hat{\boldsymbol{\theta}} + T_{\theta\theta} \hat{\boldsymbol{\varphi}}) r^2 \sin \theta dr d\varphi \quad (2.79)$$

$$= \iint_2 (-T_{\theta\varphi} [\cos \theta (\cos \varphi \hat{\mathbf{x}} + \sin \varphi \hat{\mathbf{y}}) - \sin \theta \hat{\mathbf{z}}] + T_{\theta\theta} [-\sin \varphi \hat{\mathbf{x}} + \cos \varphi \hat{\mathbf{y}}]) r^2 \sin \theta dr d\varphi. \quad (2.80)$$

Using the same reasoning as we did for the first and third surfaces and using that $\theta = \pi/2$, we see that the torque becomes

$$\langle \boldsymbol{\tau}_2^{ax} \rangle = \langle \boldsymbol{\tau}_2^{tr} \rangle = 0 \quad (2.81)$$

$$\langle \boldsymbol{\tau}_2^{cross} \rangle = \epsilon_m \pi \int_a^{a+d} [-E_r^{ax} E_r^{tr} + E_\theta^{ax} E_\theta^{tr}] r^2 dr \hat{\mathbf{y}}. \quad (2.82)$$

We solve the resulting integrals in Equations 2.77 and 2.82 numerically, for the same reason as for the integrals for the force.

If we now look at the final expression for the torque of the particle

$$\boldsymbol{\tau} = \sin \nu \cos \nu [\langle \boldsymbol{\tau}_1^{cross} \rangle + \langle \boldsymbol{\tau}_2^{cross} \rangle + \langle \boldsymbol{\tau}_3^{cross} \rangle] = \frac{1}{2} \sin 2\nu [\langle \boldsymbol{\tau}_1^{cross} \rangle + \langle \boldsymbol{\tau}_2^{cross} \rangle + \langle \boldsymbol{\tau}_3^{cross} \rangle] \hat{\mathbf{y}}, \quad (2.83)$$

we can see that it has the same form as Equation 2.2.

3

Model implementation

3.1. Solving for the coefficients of the potential

For the implementation of the model, we make separate functions to calculate the A_i^{kn} , B_i^{kn} , C_i^{kn} , D_i^{kn} and R_i^k coefficients with $i = 1, 2, 3, 4$, as we specified in Equations 2.33. If we iterate over n and k we can create the matrix and vector of Equation 2.32. We subsequently use the numpy function `numpy.linalg.solve` to solve the system of equations and to get the desired coefficients α , β , γ and δ .

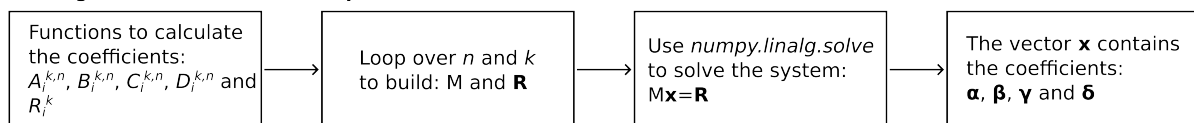
3.2. Calculating the potential with the coefficients

When we have obtained the coefficients, we can calculate the potential at all the points. First, we determine the region on the basis of the coordinates of the point, to pass the correct coefficients to the correct function. Then we determine the factors in front of the (associated) Legendre polynomials for each n and lastly we calculate the Legendre or associated Legendre polynomials using the functions `numpy.polynomial.legendre.legval` and `scipy.special.lpmv` respectively.

3.3. Calculation Force Maxwell Stress Tensor (MST)

For every surface which needs to be integrated, we create a function which calculates the integrand of the integrals given in subsection 2.2.2. The function takes only the argument of the variable which needs to be integrated and the integration is done by the scipy function `scipy.integrate.quad`.

Solving the coefficients of the potential



Calculate the potential with the coefficients

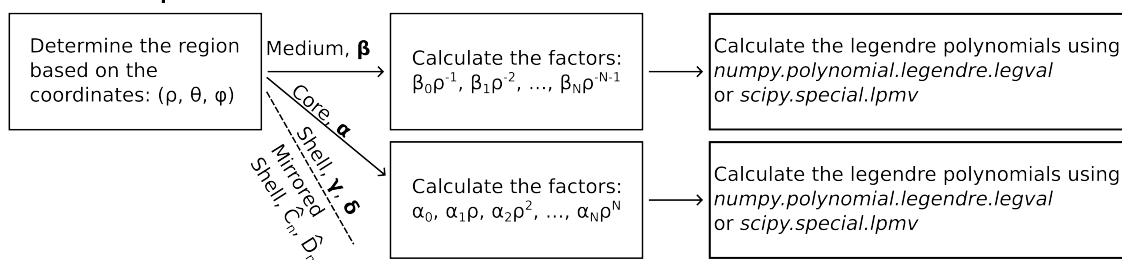


Figure 3.1: Diagram of the steps used for implementation of the model.

4

Results

In this chapter, we show the results of the calculations done using the model. First, we discuss the different calculations of the potentials, where we compare the model to known potentials cases and consider the stability of the model. After that, we show the potential and the field of the Janus particle due to an external z - and x -field. Lastly, we consider the calculations of the force and torque done using the dipole approximation or done using the Maxwell Stress Tensor method and compare them.

The calculations for the Janus particle were done with the following values, which are indicated in Figure 2.2c. For the medium the permittivity of water at $20^\circ C$ was chosen, $\epsilon_m = 80\epsilon_0$ [17], where $\epsilon_0 = 8.85 \cdot 10^{-12} \text{ Fm}^{-1}$ is the permittivity of free space. The shell was assumed to be made of TiO_2 , thus the permittivity of the shell is $\epsilon_s = 114\epsilon_0$ [18]. The core was made of SiO_2 which has a permittivity of $\epsilon_c = 3.9\epsilon_0$ [17]. We take the permittivity of the lower shell equal to the permittivity of the medium, $\epsilon_{\hat{s}} = \epsilon_m = 80\epsilon_0$. The thickness was taken as $d = 0.2a$. The core radius a and the external field strength E_e are not specified since the calculations were done with dimensionless coefficients.

4.1. Potential calculation

4.1.1. Agreement with known potentials

We can change the dielectric permittivities of the various regions, to have the model represent the cases for which the solutions are already known. If all the permittivities are equal to each other ($\epsilon_m = \epsilon_s = \epsilon_{\hat{s}} = \epsilon_c = 80\epsilon_0$), there is no particle in the medium and we will expect no change in the potential. If the permittivities of the upper and the lower shell are equal to the permittivity of the medium ($\epsilon_m = \epsilon_s = \epsilon_{\hat{s}} = 80\epsilon_0$; $\epsilon_c = 3.9\epsilon_0$) or that of the core ($\epsilon_m = 80\epsilon_0$; $\epsilon_s = \epsilon_{\hat{s}} = \epsilon_c = 3.9\epsilon_0$), we should obtain the potential of a sphere with radius a or radius $a + d$, respectively. When the permittivities of the upper shell and the lower shell are equal but they differ from the core and the medium ($\epsilon_m = 80\epsilon_0$; $\epsilon_s = \epsilon_{\hat{s}} = 114\epsilon_0$; $\epsilon_c = 3.9\epsilon_0$), the model should give the potential of a particle with a concentric shell.

In Tables 4.1 we present the values of the α_1 , β_1 , γ_1 and δ_1 coefficients, together with their expected dimensionless coefficients. We calculated the coefficients with $N = 50$ for a field pointing in the axial direction and for a field in the transverse direction. The numerically calculated coefficients with $n \neq 1$ are all 0 we do not show these values. Furthermore, $\hat{C}_n = C_n$ and $\hat{D}_n = D_n$ for all n , since $\epsilon_s = \epsilon_{\hat{s}}$, so we also do not show these values in the tables.

In Table 4.1a, Table 4.1b and Table 4.1c we provide, respectively, the results of the cases for no particle, for a spherical particle of radius a and for a spherical particle of radius $a + d$. In the tables, we can see that the coefficients calculated with the model, in both directions, are equal to the exact coefficients.

In Table 4.1d the case for the single shelled particle is shown with the two exact solutions of Jones (1995) [6] and Turcu *et al.* (1989) [14]. The data is also plotted in Figure 4.1. In the table and in the figure we can see that for the coefficients α_1 , γ_1 and δ_1 the solutions of the model are equal to the coefficients as calculated by Turcu *et al.*. On the other hand, the β_1 coefficient of the model is equal to the solution of Jones. This is the same result we saw in the solution given by Maple, Equations 2.17, and in appendix C.

Table 4.1: In this table we show different values of the first coefficients calculated by the model for cases of: no particle (a), a spherical particle with radius $r = a$ (b), a spherical particle with radius $r = a + d$ (c) and a shelled particle (d). The coefficients calculated for an external field in the axial- and the transverse-direction are shown.

(a) No particle ($\epsilon_m = \epsilon_s = \epsilon_{\hat{s}} = \epsilon_c$)

	Exact	Axial field	Transverse field
α_1	-1	-1	-1
β_1	0	0	0
γ_1	-1	-1	-1
δ_1	0	0	0

(b) Spherical particle with radius a ($\epsilon_s = \epsilon_{\hat{s}} = \epsilon_m$)

	Exact	Axial field	Transverse field
α_1	-1.46431	-1.46431	-1.46431
β_1	-0.46431	-0.46431	-0.46431
γ_1	-1	-1	-1
δ_1	-0.46431	-0.46431	-0.46431

(c) Spherical particle with radius $a + d$ ($\epsilon_s = \epsilon_{\hat{s}} = \epsilon_c$)

	Exact	Axial field	Transverse field
α_1	-1.46431	-1.46431	-1.46431
β_1	-0.80232	-0.80232	-0.80232
γ_1	-1.46431	-1.46431	-1.46431
δ_1	0	0	0

(d) Shelled particle ($\epsilon_s = \epsilon_{\hat{s}}$)

	Exact Jones (1995)	Exact Turcu <i>et al.</i> (1989)	Axial field	Transverse field
α_1	-1.28807	-1.3863	-1.3863	-1.3863
β_1	-0.34263	-0.80561	-0.34263	-0.34263
γ_1	-1.07494	-0.94001	-0.94001	-0.94001
δ_1	-0.21314	-0.44629	-0.44629	-0.44629

4.1.2. Convergence of solution

The solution of the system 2.32 tends to diverge at two points: $r = a$ and $r = a + d$. If the series 2.22 and 2.35 converge at these points, they converge everywhere [16]. To verify the convergence we solve the system for different values of N and calculate the relative error in the potential:

$$e_{\Phi} = \left| \frac{\Phi_N - \Phi_{340}}{\Phi_{340}} \right|, \quad (4.1)$$

where Φ_N is the potential calculated for N and Φ_{340} is the potential for $N = 340$. The relative error in the potential for $r = a + d$, $\theta = \pi/4$ and $\varphi = 0$ is plotted in Figure 4.2a on a logarithmic scale. We can see from the figure that the relative error has an oscillating behaviour. If we focus on the peaks of the oscillations, we can see that in both cases the error decreases for higher N , thus we can assume that the error converges further towards zero. For both the external field along the z -axis and the x -axis we see that there is a resonance-like behaviour in the error. The amplitudes of the oscillations increase toward a point, where the oscillations are at their largest and decrease beyond that point. For the external field in the z -direction, the resonance-point lies around $N = 155$ and for the external field in the x -direction that point lies around $N = 320$.

The relative error is lower than 0.01% for $N = 50$. We can get a lower error by taking a higher N , however, this will result in a longer computation time. So for this report, the figures and the values we present are calculated with $N = 50$.

Since we use the dipole term, β_1 , for the calculation of the torque, we also consider the relative error of β_1 : e_{β_1} . The relative error is calculated in the same way as Equation 4.1 but with $\beta_{1,N}$ as the dipole term calculated for N and $\beta_{1,340}$ as the dipole term calculated for $N = 340$. The results are plotted in Figure 4.2b. We can see in the figure that the error in the dipole coefficient decreases faster than the error in the potential. Furthermore, there is no oscillatory behaviour in the error. For the dipole term we can see that, in both cases, the error is below 0.01% for $N = 50$. Thus $N = 50$ is also sufficient for the dipole calculations of the torque. In

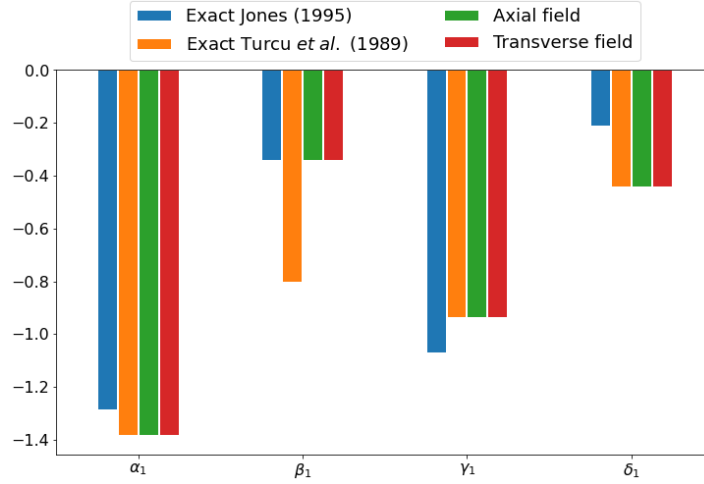


Figure 4.1: Barplot of the coefficients for the shelled particle, as calculated by Jones (1995) and Turcu *et al.* (1989) and calculated with the model for an external field in the axial direction and the transverse direction.

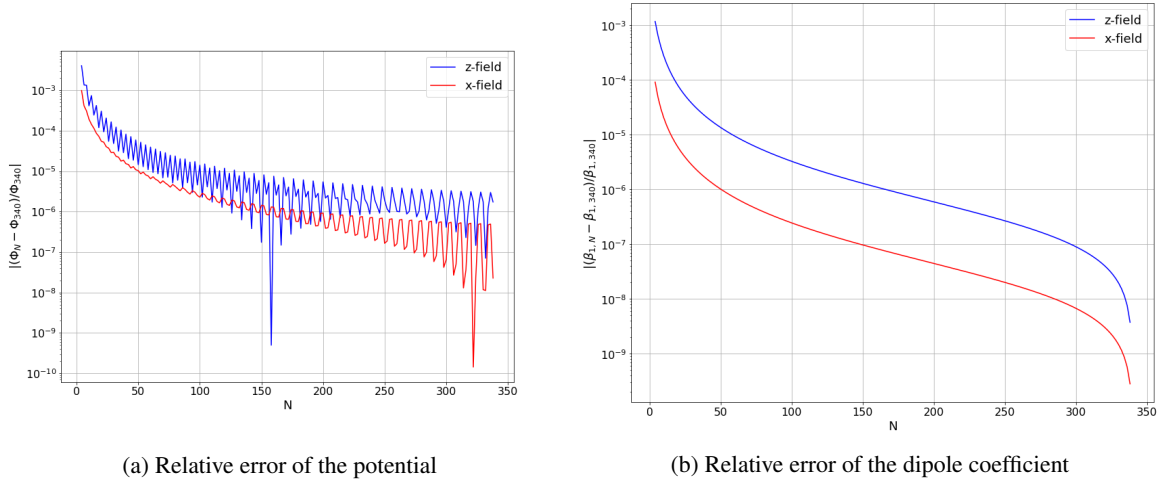


Figure 4.2: Plots of the relative errors of the potential value at ($r = a$, $\theta = \pi/4$, $\varphi = 0$) and the dipole coefficient calculated for different values of N . The plots are shown on a logarithmic scale. The relative errors are shown for both the axial and transverse field direction.

Figure D.1 the relative errors of the α_1 , γ_1 and δ_1 are shown. In these plots we see the same behaviour as we see for β_1 in Figure 4.2b.

4.1.3. Potential Janus particle

In Figure 4.3 and Figure 4.4 we show the potential and the resulting fields of a Janus particle for an external axial and transverse field respectively. The fields were calculated using the Equations 2.50 and 2.51 and converted to Cartesian coordinates using Equations 2.52. In these figures, we have that $\varphi = 0$, for $x \geq 0$, or $\varphi = \pi$, for $x < 0$, thus $E_y = 0$ for all points in the plane shown in the axial and the transverse case, hence, this field is not shown in the figures.

In the fields of the axial and transverse cases we can see some similarities. First, if we compare the field in the direction perpendicular to the external field, the x -field for the axial case and the z -field for the transverse case, we can see that the fields have the same shape. Both the fields have a butterfly-pattern, with the upper-left and lower-right "wings" having a positive field and the lower-left and upper-right being negative. For the fields along the direction of the external field we can see that the field is the weakest outside the core along the direction of the field. The field is the strongest in the direction perpendicular to the applied field.

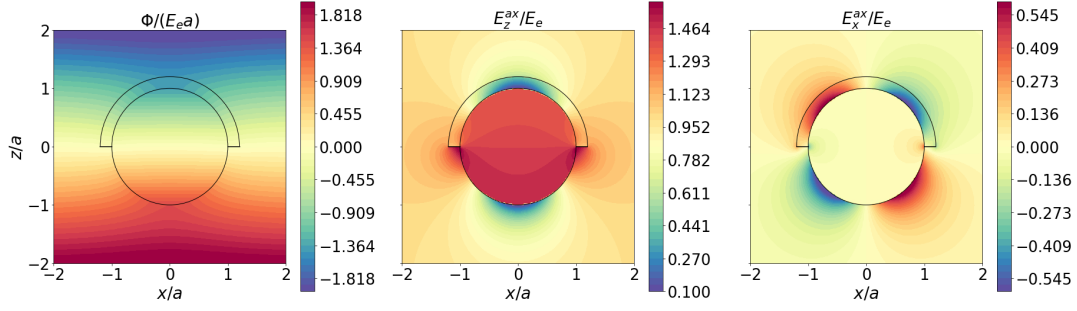


Figure 4.3: Plots of the potential and the field in the z - and x -directions for a Janus particle in an axial-oriented electric field, shown in the left middle and right plots respectively.

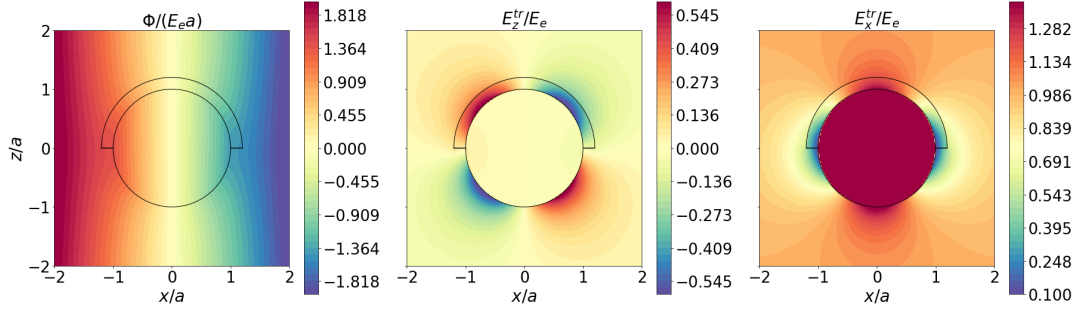


Figure 4.4: Plots of the potential and the field in the z - and x -directions for a Janus particle in an transverse-oriented electric field, shown in the left middle and right plots respectively.

4.2. Calculation of force and torque

4.2.1. Dipole approximation

As we already discussed in subsection 2.2.1, there is no force on the dipole due to the external field being uniform. There is, however, a torque on the particle in the dipole approximation. In Figure 4.5 we show the torque for different values of the angle ν . If the torque is positive, the particle will turn counterclockwise and thus the angle ν will decrease. On the other hand, if the torque is negative, the particle will turn clockwise and the angle ν will increase. Thus, we can see that for $\nu = \pi/2$ we have a stable equilibrium. This angle corresponds to the position where the field is pointing in the positive x -direction as shown in Figure 2.1. We can also deduce that there is a stable equilibrium when the field is pointing in the negative x -direction. This corresponds to the angle $\nu = -\pi/2$. The angles $\nu = 0$ and $\nu = \pi$, which correspond to the applied field in the positive or negative z -direction, are thus unstable equilibriums.

4.2.2. Maxwell Stress Tensor (MST)

In Tables 4.2 we show the results of the calculations of the force and torque. Table 4.2a shows the axial contribution of the force, Table 4.2b shows the transverse contribution of the force and Table 4.2c the contribution of the cross term to the force. In Table 4.2d the contribution of the cross term to the torque is shown. The torques due to the axial term and the transverse terms are not shown since they are zero. In both the tables, we first display contributions for each surface and finally the total force or torque on the particle.

We can see that the transverse component of the force has the smallest magnitude and the cross-component has the largest magnitude. Because we have that the transverse and the axial component are both positive, we see that the Janus particle will always want to move in the direction its cap is pointing. This is regardless of the direction of the field due to the squared sine and cosine in Equation 2.72. For the cross-component of the force we have that due to the $\sin \nu \cos \nu$, the particle will have a force in the positive x -direction for the angles $0 < \nu < \pi/2$ and $\pi < \nu < 3\pi/2$. The particle will have a force in the negative x -direction for the other angles.

In the dipole approximation, we saw that there was no force on the particle, however, there is a force on the particle according to the Maxwell Stress Tensor. Nevertheless, we have that the forces on the separate surfaces almost cancel each other. Since the resulting forces, for the axial, transverse and cross-components, are three orders of magnitude lower than their respective the largest force on an individual surface.

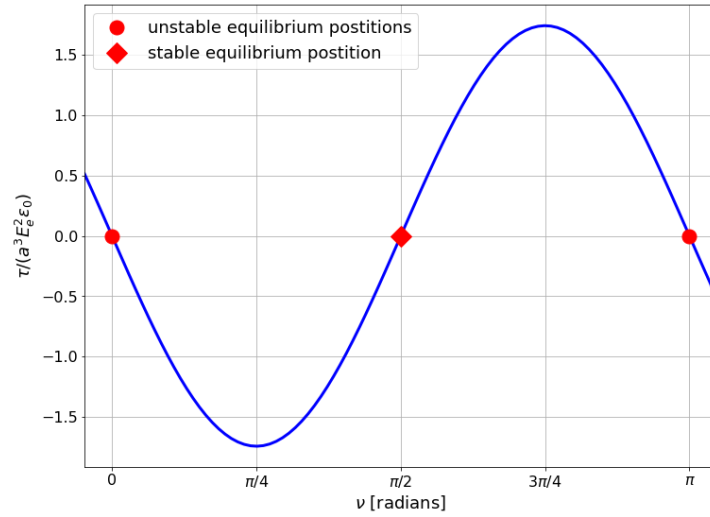


Figure 4.5: A plot of the torque on the Janus particle for different field angles ν . The stable position is denoted with a diamond and lies at $\nu = \pi/2$, this position corresponds to the field pointing in the positive x -direction. The unstable positions are denoted with a circle and lie at $\nu = 0$ and $\nu = \pi$, which correspond to a field pointing in the positive and negative z -direction, respectively.

We see that the cross-component of the torque on the particle is negative, which is the same as in the dipole approximation. So we have the same shape of the torque as in Figure 4.5. Thus we have that for angle $\nu = \pi/2$ the particle is at a stable equilibrium. In the dipole approximation we have that $[\chi_{ax} - \chi_{tr}]E_e^2 = -3.484a^3E_e^2\epsilon_0$, which is close to the value of the torque calculated by the Maxwell Stress Tensor.

Thus the dipole approximation is a reasonable approximation to calculate the force and torque on a Janus particle. However this is only for the specific parameters used in this report, we for example expect that these values for the torque and force will have larger differences if the thickness d is increased. Because, in that case the model is less similar to the model of a sphere, which is perfectly described by a dipole.

Table 4.2: Force in the z -direction on the Janus particle for an axial external field (a) and for a transverse external field (b). The first three entries in the tables are the forces for each individual surface and the last entry is for the total force.

(a) Axial force		(b) Transverse force	
	Force/ $(a^2 E_e^2 \epsilon_0)$ in the z -direction		Force/ $(a^2 E_e^2 \epsilon_0)$ in the z -direction
$\langle F_1^{ax} \rangle$	5.373836	$\langle F_1^{tr} \rangle$	-252.898
$\langle F_2^{ax} \rangle$	-134.019	$\langle F_2^{tr} \rangle$	50.03007
$\langle F_3^{ax} \rangle$	128.7616	$\langle F_3^{tr} \rangle$	202.8756
$\langle F^{ax} \rangle$	0.115974	$\langle F^{tr} \rangle$	0.008121

(c) Cross force		(d) Cross torque	
	Force/ $(a^2 E_e^2 \epsilon_0)$ in the x -direction		Torque/ $(a^3 E_e^2 \epsilon_0)$ in the y -direction
$\langle F_1^{cross} \rangle$	278.6593	$\langle \tau_1^{cross} \rangle$	3.835102
$\langle F_2^{cross} \rangle$	-137.672	$\langle \tau_2^{cross} \rangle$	-6.3761
$\langle F_3^{cross} \rangle$	-140.217	$\langle \tau_3^{cross} \rangle$	-0.82279
$\langle F^{cross} \rangle$	0.770905	$\langle \tau^{cross} \rangle$	-3.36379

5

Conclusion

The purpose of this report was to derive a semi-analytic description of the force and torque on a Janus particle due to an electric field. We derived this solution by first finding the potential because of the electric field and then calculating the force and torque with the dipole approximation and the Maxwell Stress Tensor.

The model of the Janus particle has been developed by adapting the approach developed by Scherbak *et al.* (2015) [15]. If the model is reduced to the case of a spherical particle or a spherical particle with a concentric shell, then the potential calculated using the model corresponds with the known potential of those cases. The solution of the model on the boundaries is stable and converges for a higher number of terms in the series, thus the solution converges everywhere. The values of the dipole coefficient, which we use for the dipole approximation, also converge for a higher number of terms.

In the dipole approximation, we saw that there is no force on the Janus particle since the applied field is uniform. There is, however, torque on the Janus particle, which has resulted that the particle orients its axis perpendicular to the direction of the electric field. The force calculated with the Maxwell Stress Tensor method is non zero, but the magnitude of the total force is three orders of magnitude than the separate components of the force. The torque calculated with the stress tensor is approximately equal to the torque as calculated with the dipole approximation.

Our study only focused on developing the model to calculate the force and torque. We did not investigate the effects of different parameters or the use of more complicated electric fields for rotation of the particle. Thus we recommend researching at which parameter configurations the agreement between the dipole approximation and the Maxwell Stress Tensor breaks down. We expect that this happens for a larger shell thickness, however, this can possibly happen for varying permittivities. Furthermore, we recommend using the model from this report to investigate how to rotate the Janus particle without displacing it. This is not trivial since there is always a force, although small, pointing in the direction the cap of the particle is pointing. This can possibly be done by using a rotating external electric field. Another approach to research is to calibrate the strength of the external field such that there is enough torque to turn the particle but the force is not large enough to move the particle.

Bibliography

- [1] Andreas Walther and Axel H.E. Müller. Janus particles. *Soft Matter*, 4(4):663–668, 3 2008.
- [2] Yu Zhang, Nathaniel K. Grady, Ciceron Ayala-Orozco, and Naomi J. Halas. Three-dimensional nanostructures as highly efficient generators of second harmonic light. *Nano Letters*, 11(12):5519–5523, 12 2011.
- [3] Nicholas S. King, Yang Li, Ciceron Ayala-Orozco, Travis Brannan, Peter Nordlander, and Naomi J. Halas. Angle- and spectral-dependent light scattering from plasmonic nanocups. *ACS Nano*, 5(9):7254–7262, 9 2011.
- [4] Daniel Mann, Stefanie Voigt, Ryan Van Zandvoort, Helmut Keul, Martin Möller, Marcel Verheijen, Daniel Nascimento-Duplat, Man Xu, H. Paul Urbach, Aurèle J.L. Adam, and Pascal Buskens. Protecting patches in colloidal synthesis of Au semishells. *Chemical Communications*, 53(27):3898–3901, 3 2017.
- [5] Michael Pycraft Hughes. AC electrokinetics: applications for nanotechnology. *Nanotechnology*, 11(2):124, 6 2000.
- [6] Thomas B. Jones. *Electromechanics of Particles*. Cambridge University Press, 10 1995.
- [7] Morgan Hywel and Nicolas G. Green. *AC Electrokinetics: Colloids and Nanoparticles Microtechnologies and microsystems series*. page 324, 2003.
- [8] Wei Lu. *Orientation of core-shell nanoparticles in an electric field*. 2007.
- [9] Koji Asami, Tetsuya Hanai, and Naokazu Koizumi. Dielectric approach to suspensions of ellipsoidal particles covered with a shell in particular reference to biological cells. *Japanese Journal of Applied Physics*, 19(2):359–365, 2 1980.
- [10] Yu-Liang Chen and Hong-Ren Jiang. Electrorotation of a metallic coated Janus particle under AC electric fields. Cite as: *Appl. Phys. Lett*, 109:191605, 2016.
- [11] Behrouz Behdani, Kun Wang, and Carlos A Silvera Batista. Electric polarizability of metallodielectric Janus particles in electrolyte solutions †. Cite this: *Soft Matter*, 17:9410, 2021.
- [12] Xujing Wang, Xiao Bo Wang, and Peter R.C. Gascoyne. General expressions for dielectrophoretic force and electrorotational torque derived using the Maxwell stress tensor method. *Journal of Electrostatics*, 39(4):277–295, 8 1997.
- [13] LAPLACE’S EQUATION IN SPHERICAL COORDINATES With Applications to Electrodynamics.
- [14] I. Turcu and C. M. Lucaciu. Dielectrophoresis: a spherical shell model. *Journal of Physics A: Mathematical and General*, 22(8):985, 4 1989.
- [15] S. A. Scherbak, O. V. Shustova, V. V. Zhurikhina, and A. A. Lipovskii. Electric Properties of Hemispherical Metal Nanoparticles: Influence of the Dielectric Cover and Substrate. *Plasmonics*, 10(3):519–527, 6 2015.
- [16] Henrik Kettunen, Henrik Wallín, and Ari Sihvola. Polarizability of a dielectric hemisphere. *Journal of Applied Physics*, 102(4):044105, 8 2007.
- [17] Engineering ToolBox. *Relative Permittivity - the Dielectric Constant*, 2010.
- [18] H. Ozaki, M. Kurimoto, T. Sawada, T. Funabashi, T. Kato, and Y. Suzuoki. Evaluation of relative permittivity and coefficient of thermal expansion of TiO₂/SiO₂ epoxy composites for permittivity-graded insulator. *Annual Report - Conference on Electrical Insulation and Dielectric Phenomena, CEIDP, 2017-October*:568–571, 1 2018.

A

Python code

The Python code used for this report is available at

<https://gitlab.tudelft.nl/optica/force-and-torque-on-janus-particle>

We implemented the solver of the coefficients in `potential_calculation.py`. Also, the functions to calculate the value of the potential and the field from the coefficients are defined in that file. The file calls the functions in `build_u_matrix.py`, which calculate the values of $U_{n,k}$ or $U_{n,k}^1$. In the file `input_file.py` we defined a dictionary called `variables` in which the variables for the model are defined. All the other files import the variables dictionary from the input file, thus there is a central place to modify the input of the model. In `plotting.py` we have some standard functions for visualizations defined, such as the function to draw the outline of a Janus particle.

The files which start with `error_in_potential` calculate the coefficients of their respective cases: no particle, a spherical particle or a single shelled particle.

The script in `calculate_potential_coeff_diff_N.py` calculates the values of the coefficients and the potential at a point for multiple values of N and stores the data in `Data/`. The files `plot_convergence_coeff.py` and `plot_convergence_potential.py` use the saved data to plot the relative error of the α_1 , β_1 , γ_1 and δ_1 coefficients and the relative error of the potential, respectively. The other files starting with `plot` are files that plot the figures we show in this report.

Finally, we have in the files `mst_force_janus_particle.py` and `mst_torque_janus_particle.py` the code that calculates the force and torque with the Maxwell Stress Tensor method.

B

Nomenclature

Table B.1: Table with the names of the variables and constants used throughout the report

E_e	External electric field [V/m]
\mathbf{p}	Dipole moment [Cm]
\mathbf{F}	Force [N]
$\boldsymbol{\tau}$	Torque [Nm]
Φ	Electric potential [V]
P_n	Legendre polynomial
P_n^1	Associated Legendre polynomial
a	core radius [m]
d	shell thickness [m]
(r, θ, φ)	Spherical coordinates
$\rho = r/a$	Dimensionless radius
$\xi = \cos\theta$	Variable Legendre polynomial
$\zeta = 1 + d/a$	Dimensionless outer radius
ϵ	Electric permittivity [Fm]
N	Cut-off term series
$\langle . \rangle$	Time averaging
subscript: m	medium
subscript: s	shell
subscript: \hat{s}	mirrored shell
subscript: c	core

C

Comparison solutions shelled particle

To investigate the difference in the solutions given by Jones (1995) and Turcu *et al.* (1989) the potential and the displacement field in the core, shell and medium are plotted in Figures C.1. As a reminder, the coefficient corresponding to the core is A , the coefficients corresponding to the shell are C and D and the coefficient corresponding to the medium is B .

In Figure C.1a, we plot the potential across the shell. We can see that for the solution of Jones the potential is continuous across the boundaries. However, the solution of Turcu *et al.* is not continuous at the shell-medium boundary, but it is continuous with the solution of Jones at that boundary. In Figure C.1a we show the displacement field, ϵE , across the shell. The figure illustrates that the displacement field is discontinuous at both boundaries for the Jones solution. On the other hand, the field given by Turcu *et al.* is continuous at the core-shell boundary, but discontinuous at the shell-medium boundary. We notice that the solution of Turcu *et al.* is continuous with the Jones solution at the shell-medium boundary. This implies that the correct solution is the solution with the A , C and D coefficients of Turcu *et al.* and the B coefficient of Jones, which is the same answer Maple gives as shown in Equations 2.17.

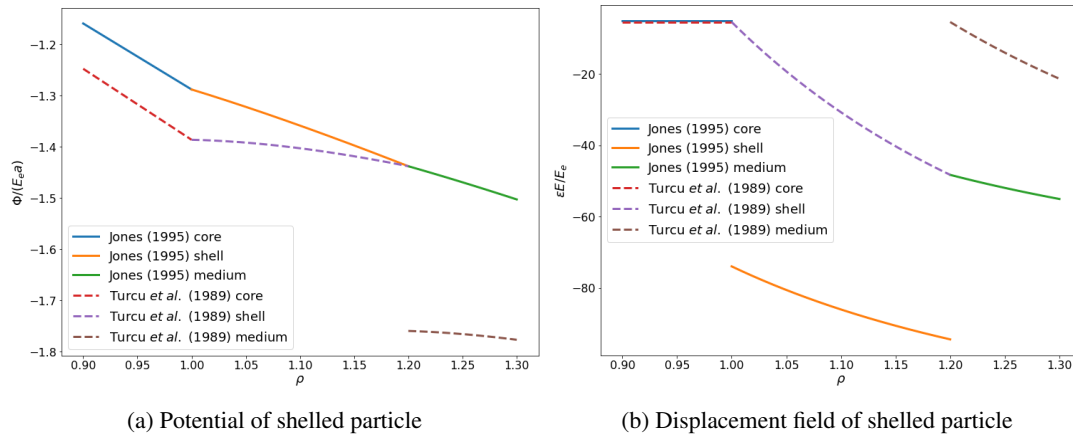


Figure C.1: Plots of the values of the potential and the displacement field, ϵE , across the shell according to the solutions of Jones (1995) [6] and Turcu *et al.* (1989) [14].

D

Relative error n=1 coefficients

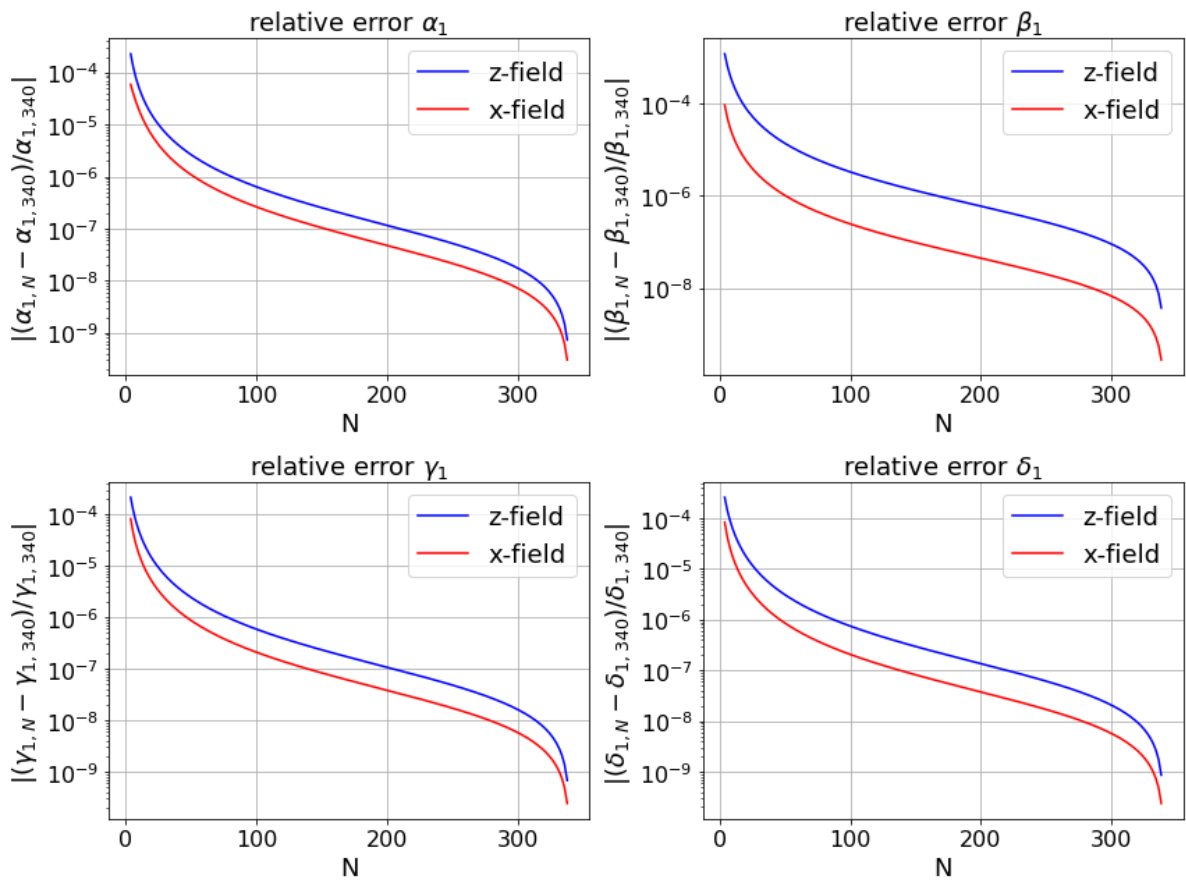


Figure D.1: Relative error of the coefficients α_1 , β_1 , γ_1 and δ_1 plotted for different values of N .